

Positioning Estimation of Radiating Sources using the Multiple Signal Classification (MUSIC) Technique

MUHAMMAD SALEM¹, MUJAHID AL-AZZO²

Electronics Engineering Department
Ninevah University
Mosul, IRAQ

Abstract: - This study used two algorithms to determine the positions of wave radiation sources. The classic Fourier transform (FT) algorithm is compared with the modern Multiple Signal Classification (MUSIC) algorithm. Both methods were implemented to estimate the positions of a single source and two sources with and without noise. The percentage error in sources' positioning resulting from spectral estimating algorithms was calculated. Moreover, the minimum separation (dpt) between transmitting sources was determined, representing the shortest distance between sources at which the algorithm can distinguish between sources and estimate their positions. Simulation results indicate that the MUSIC algorithm surpasses the FFT algorithm in enhancing positioning estimation for wave-transmitting sources.

Key-Words: - Spectral Analysis, Positioning Estimation, Uniform Linear Array (ULA), Multiple Signal Classification (MUSIC) algorithm.

Received: March 11, 2024. Revised: October 16, 2024. Accepted: November 10, 2024. Published: December 18, 2024.

1 Introduction

The problem of positioning wave radiation sources is of significant interest, particularly within communications, digital signal processing, medical technology, radar, sonar, and seismic applications. The position of the wave transmitter is determined spatially relative to a reference point, [1]. Transmitted signals are affected by random noise; typically, AWGN stands for additive white Gaussian noise, [2].

Array signal processing optimizes sensor outputs in antenna arrays to enhance system performance compared to a single antenna. It has the advantages of increased signal-to-noise ratio (SNR), side-lobe control, and improved array resolution. A uniform linear array (ULA) increases the received signal gain, [3].

The continuous-time signals received by the array antenna are converted to discrete domains for processing, [4]. To get the desired results, array processing requires an understanding of either a reference signal or the direction of the signal's source, [5]. ULA receives electromagnetic (EM) or sound waves [6].

As applications evolved, so did interest in calculating spatial characteristics. Array signal

processing employs sensors to sample a wave field and infer spatial information from source signals, [7]. Spectral estimation techniques, either parametric (modern algorithm) or non-parametric (classical algorithm), estimate a signal's spectral density from samples based on application needs [8].

Nonparametric or classical method approaches make use of Cooley and Tukey's fast Fourier transform (FFT). They are quick and simple to implement but lack accuracy and suffer from spectrum leakage, reducing result quality. They are also very sensitive to noise, which limits their effectiveness in noisy signal environments, [9], [10], [11].

Parametric methods, also known as high-resolution or subspace methods, include a multiple signal classification (MUSIC) algorithm by Schmidt. They offer high resolution, low spectral leakage, and reduced noise sensitivity, [12], [13], [14]. However, the metric superiority or the degree of the superiority is studied in this paper for the applications of finding the distance of each source from a reference axis, as well as the separation between them. In general, this can be extended to the reflecting objects as well as the transmitting sources for both ultrasonic and electromagnetic waves.

This research suggests employing parametric approaches based on eigenanalysis to address the constraints of FFT algorithm-based nonparametric methods, [15].

2 Field Analysis

Let $F(q)$ represent the field of the transmitting wave source on the transmitting axis. Let $\mathcal{H}(g)$ represent the field received from the source on the receiving axis as in Fig. 1.

$$\mathcal{H}(g) = \frac{k}{\zeta\lambda} \int_q F(q) e^{(j\beta\eta(q,g))} dq \quad (1)$$

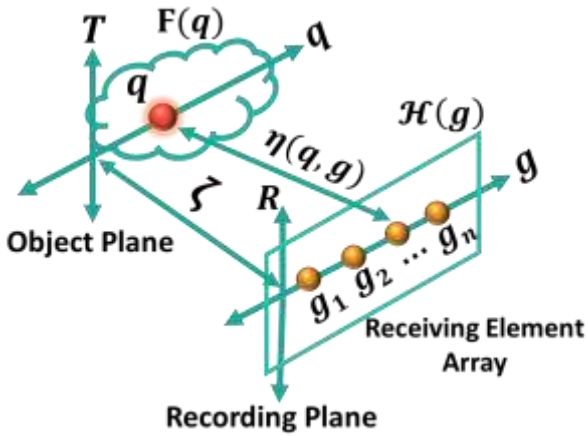


Fig. 1 Coordinate system between transmitter (T_x) and receiver (R_x).

Equation (1) very closely resembles the Fresnel principle, where β represents the wave number ($\beta = \frac{2\pi}{\lambda}$), λ represents wavelength, k is a constant, and ζ indicates the axial distance between the transmitter (object plane) and receiver (recording plane). The distance η between a point g on the recording axis (acting as an antenna) and a point q on the object axis is calculated by:

$$\eta(q, g) = \sqrt{\zeta^2 + (g - q)^2} \quad (2)$$

Using the paraxial approximation with the Fresnel region, equation (1) can be simplified to (3):

$$\mathcal{H}(g) = k_1 e^{\left(\frac{j\beta g^2}{2\zeta}\right)} \int_q F(q) e^{\left(\frac{j\beta q^2}{2\zeta}\right)} e^{\left(\frac{-j\beta qg}{\zeta}\right)} dq \quad (3)$$

Where k_1 is a complex constant obtained by simplifying equations (1) and (2) [16], [17], [18].

3 Data Model

Consider U elements of a uniform linear array (ULA) separated evenly by distance d . Consider the received signals as complex exponentials, with $\mathbf{n}(t)$ representing AWGN noise with a variance σ^2 and a mean of zero. Assume the narrowband signals are emitted by M sources that impinge on a ULA, and the source signals are expressed by $\mathbf{s}(t)$. Let the number of signal sources be less than the number of antenna elements ($M < U$). The signals received at a ULA output are as follows:

$$\mathbf{r}(t) = \mathbf{A}\mathbf{s}(t) + \mathbf{n}(t) \quad (4)$$

Where $\mathbf{r}(t) = [r_1(t), r_2(t), \dots, r_u(t)]^T$ is a vector received by the (ULA); T denotes the transpose of a matrix, and $\mathbf{s}(t) = [s_1(t), s_2(t), \dots, s_M(t)]^T$.

Where $\mathbf{n}(t) = [n_1(t), n_2(t), \dots, n_u(t)]^T$ is a noise vector, $\mathbf{A} = [\mathbf{a}(\phi_1), \mathbf{a}(\phi_2), \dots, \mathbf{a}(\phi_M)]$ and $\mathbf{a}(\phi_M) = [1, e^{\frac{-j2\pi d q_m}{\lambda \zeta}}, e^{\frac{-j4\pi d q_m}{\lambda \zeta}}, \dots, e^{\frac{-j2\pi d q_m (u-1)}{\lambda \zeta}}]^T$ is the positioning vector of the array, and it is shown in equation (5) [19], [20].

$$\mathbf{A} = \begin{bmatrix} 1 & 1 & \dots & 1 \\ e^{-j\phi_1} & e^{-j\phi_2} & \dots & e^{-j\phi_M} \\ \vdots & \vdots & \ddots & \vdots \\ e^{-j\phi_1(U-1)} & e^{-j\phi_2(U-1)} & \dots & e^{-j\phi_M(U-1)} \end{bmatrix} \quad (5)$$

3.1 Non-parametric method (Fourier transform)

The discrete Fourier transform (DFT) represents finite-length sequences, an easy function of an integer variable, k . The M -point DFT for a finite-length sequence $y(m)$ of length M that equals zero outside of the interval $[0, M - 1]$ is:

$$X_K = \sum_{m=0}^{M-1} y_m e^{\frac{-j2\pi km}{M}} \quad (6)$$

Where $k = 0, 1, 2, \dots, M-1$, and X_K is the k^{th} coefficient of the DFT, which is often complex, and y_m refers to the m^{th} sample of the time sequence and involves M samples.

The inverse discrete Fourier transform (IDFT) is the common inverse of the DFT, and the following equation may describe it:

$$Y_m = \frac{1}{M} \sum_{k=0}^{M-1} X_K e^{\frac{j2\pi km}{M}} \quad (7)$$

The fast Fourier transform (FFT) is a method for efficiently obtaining DFT that considerably reduces calculation time by calculating DFT coefficients iteratively, [21].

3.2 Music method

This algorithm separates the observation space into two subspaces: signal and noise subspaces. Equation (4)'s array output is used, and the incoming signals' covariance matrix is stated below, [22], [23], [24]:

$$C_x = E\{\mathbf{r}\mathbf{r}^H\} = \mathbf{A}\mathcal{R}_s\mathbf{A}^H + \sigma^2\mathbf{J} \quad (8)$$

Here, $E\{\cdot\}$ is the statistical expectation, \mathbf{H} represents Hermitian transpose, \mathcal{R}_s indicates the covariance matrix of signal elements, σ^2 indicates the covariance of noise elements, and \mathbf{J} is the identity matrix.

$$\mathcal{R}_s = E\{\mathbf{s}(\mathbf{t})\mathbf{s}(\mathbf{t})^H\} \quad (9)$$

The eigenvalue decomposition (EVD) approach is utilized to split the covariance matrix of incoming signals into eigenvalues and eigenvectors. The eigenvalues of C_x are $[\lambda_0, \lambda_1, \dots, \lambda_{U-1}]$, where λ_0 is the highest eigenvalue and found using:

$$|C_x - \lambda_i\mathbf{J}| = 0 \quad i = 0, 1, \dots, U - 1 \quad (10)$$

The eigenvectors of an eigenvalue λ_i are indicated as \mathbf{v}_i as follows:

$$|C_x - \lambda_i\mathbf{J}| \mathbf{v}_i = 0 \quad (11)$$

Eigenvectors related to the $U-M$ lowest eigenvalues are calculated using (12):

$$\mathbf{A}\mathcal{R}_s\mathbf{A}^H \mathbf{v}_i = 0 \quad (12)$$

Here $i = M; M+1, \dots, U-1$ is an eigenvector representing noise. Equation (13) shows that the eigenvectors related to the $U-M$ eigenvalues are orthogonal to the positioning vector \mathbf{a} . Positions are determined by detecting peaks in the spatial spectrum with the formula:

$$P_{\text{music}}(\mathbf{q}) = \frac{1}{\mathbf{a}^H \mathbf{v}_n \mathbf{v}_n^H \mathbf{a}} \quad (13)$$

Where \mathbf{a} : positioning vector and \mathbf{v}_n : Noise vector.

4 Simulation Results:

This paper studies the position estimation problem for a single source and two sources. Using simulated

data, the spatial position of the transmitter is determined relative to a reference point, where two algorithms, FFT and MUSIC, have been implemented. The study and simulation were conducted using MATLAB to achieve the desired results.

A variety of parameters were utilized, including η (number of samples or number of antennas), γ (wavelength), ζ (distance between transmitter and receiver axes), Δs (sampling interval or distance between antennas), and P_{S1} (the position of the first source) and P_{S2} (the position of the second source). The study uses different values of some parameters to obtain a wide range of results.

The percentage error (E_{PS}) in the sources' position for all methods can be determined using the following equation:

$$E_{PS} = \frac{|P_{S(\text{actual})} - P_{S(\text{Reconstructed})}|}{P_{S(\text{actual})}} * 100 \% \quad (14)$$

$P_{S(\text{actual})}$ is the actual (or real) position, and $P_{S(\text{Reconstructed})}$ is the value of the sources' position obtained after processing.

The minimum separation (dpt) between transmitting sources was determined, representing the shortest distance between sources at which the algorithm can distinguish between sources and estimate their positions, and is calculated using the following equation:

$$\text{Min. Separation (dpt)} = P_{S2} - P_{S1} \quad (15)$$

The minimum separation (dpt) In (cm).

4.1 Results without noise:

4.1.1 Simulation results with a single source:

A single transmitting source is used. It emits a signal with wavelength ($\gamma = 0.4$ cm). Using the parameters $P_{S1} = 2$ cm, $\Delta s = 1$ cm, $\zeta = 50$ cm, and $\eta = 10$, Fig. 2 shows that the FFT algorithm (red line) estimates the position of the source at $PS1 = 2.109375$ cm, with a percentage error of $E_{PS} = 5.47\%$ from the actual source position $P_{S1} = 2$ cm.

In contrast, the MUSIC algorithm (blue line) estimates the position at $P_{S1} = 2.0313$ cm, with a percentage error of $E_{PS} = 1.56\%$, significantly lower than the FFT algorithm. Additionally, the main lobe width was narrower, and side lobes (SL) levels were nonexistent, enhancing the accuracy of the position

estimation and reducing power loss compared to the FFT algorithm.

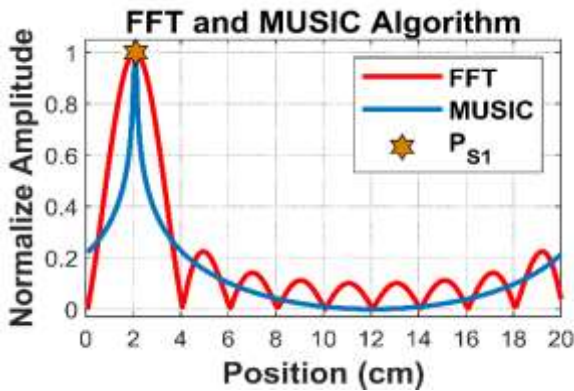


Fig. 2 Position estimation for a single source using the FFT and MUSIC algorithms $P_{S1} = 2$ cm, $\gamma = 0.4$ cm, $\Delta s = 1$ cm, $\zeta = 50$ cm, and $\eta = 10$.

Fig. 3 illustrates the relationship between the percentage error (E_{PS}) and η for a single source after implementing the FFT and the MUSIC algorithms. The figure shows that the MUSIC algorithm outperforms the FFT algorithm with lower E_{PS} in estimating the source position. The results indicated that increasing η does not affect E_{PS} .

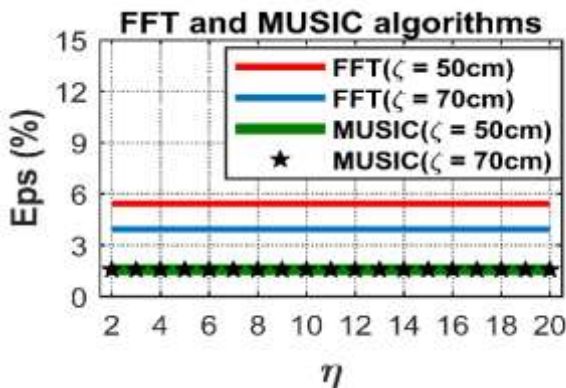


Fig. 3 The relationship between the percentage error (E_{PS}) and η using the FFT and MUSIC algorithms $P_{S1} = 2$ cm, $\gamma = 0.4$ cm, $\Delta s = 1$ cm.

4.1.2 Simulation results with two sources:

The FFT and MUSIC algorithms are applied to estimate the position of two sources using the same parameters as for a single source. The minimum separation (d_{pt}) and E_{PS} for each source are calculated.

Using the parameters $P_{S1} = 2$ cm, P_{S2} is changed until obtaining a minimum detectable distance d_{pt} , $\gamma = 0.4$ cm, $\Delta s = 1$ cm, $\zeta = 50$ cm, and $\eta = 10$, Fig. 4 (a) illustrates the performance of the FFT algorithm with

two signal sources. The algorithm fails to distinguish between the sources when they are close to each other ($d_{pt} = 1.35$ cm), as their peaks merge, and it becomes difficult to differentiate between them.

While the FFT algorithm in Fig. 4 (b) succeeded in distinguishing between the sources after increasing the distance between them ($d_{pt} = 1.59$ cm), the first source's position was estimated at $P_{S1} = 1.640625$ cm with $E_{PS1} = 17.97\%$, and the second source's position was estimated at $P_{S2} = 4.0625$ cm with $E_{PS2} = 13.16\%$, with many and considerable SL levels and wide main lobes.

In contrast, the MUSIC algorithm in Fig. 4 (c) successfully distinguishes the sources with high accuracy ($d_{pt} = 0.45$ cm), estimating the position of the first source at $P_{S1} = 2.0313$ cm with $E_{PS1} = 1.56\%$ and the position of the second source at $P_{S2} = 2.4219$ cm with $E_{PS2} = 1.15\%$, which is much lower than the FFT algorithm. Additionally, the main lobe width was narrower, and SL levels were minimal, enhancing the accuracy of sources' position estimation and reducing power loss compared to the FFT algorithm.

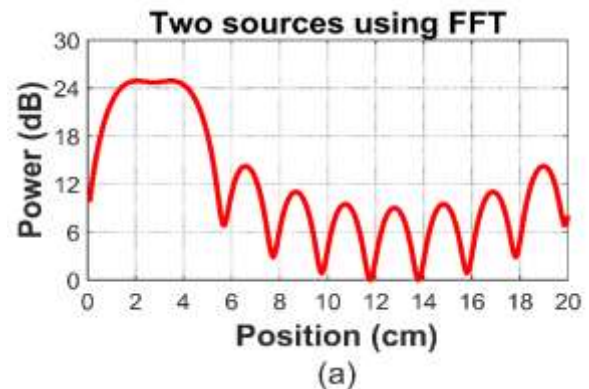


Fig. 4 (a) Shows the failure of the FFT algorithm to distinguish between sources.

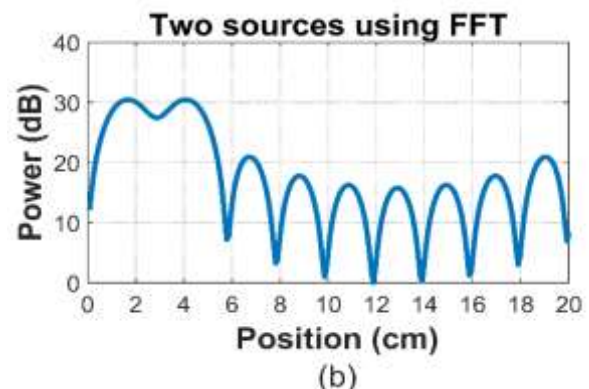


Fig. 4 (b) Shows the success of the FFT algorithm in distinguishing between sources.

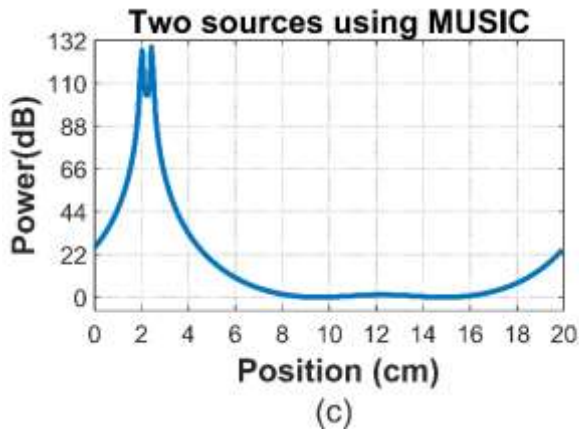


Fig. 4 (c) Shows the success of the MUSIC algorithm in distinguishing between sources.

After implementing the FFT and MUSIC algorithms, Fig. 5 illustrates the relationship between minimum separation (dpt) and η for two sources. The figure shows that the MUSIC algorithm outperforms the FFT algorithm by distinguishing between very close sources (high resolution). The results indicated that two parameters affect dpt, namely ζ and η . The dpt increases with the increase in ζ (requiring greater distance between sources for distinguishing) and decreases with increased η . Therefore, $\zeta = 50$ cm is better than $\zeta = 70$ cm, and so on.

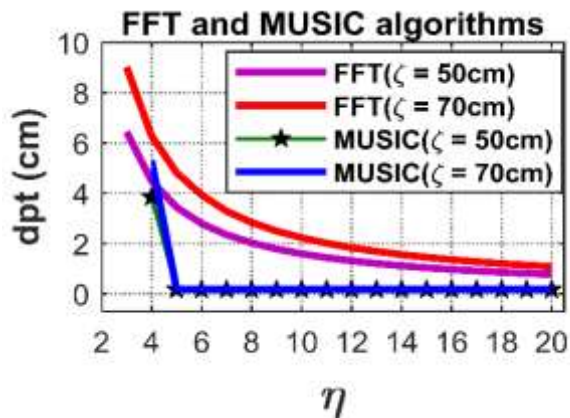


Fig. 5 The relationship between minimum separation (dpt) and η using the FFT algorithm and MUSIC algorithm $P_{S1} = 2$ cm, $P_{S2} =$ variable, $\gamma = 0.4$ cm, $\Delta s = 1$ cm.

Fig. 6 (a and b) illustrates the relationship between the percentage error (E_{PS}) and η for two sources after implementing the FFT and MUSIC algorithms. The figure indicates that the MUSIC algorithm outperforms the FFT algorithm with lower E_{PS} in estimating sources' positions. The results suggest that E_{PS} decreases with increasing η . Additionally, the E_{PS} for the second source (E_{PS2}) is

less than that of the first source (E_{PS1}), indicating that the position estimation of the second source is more accurate.

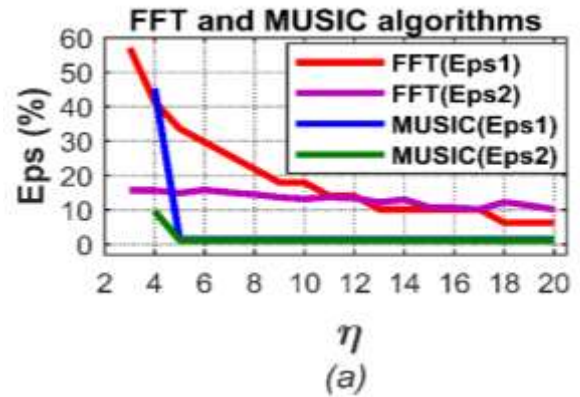


Fig. 6 (a) The relationship between the percentage error (E_{PS}) and η using the FFT and MUSIC algorithms $P_{S1} = 2$ cm, $P_{S2} =$ variable, $\gamma = 0.4$ cm, $\Delta s = 1$ cm, $\zeta = 50$ cm.

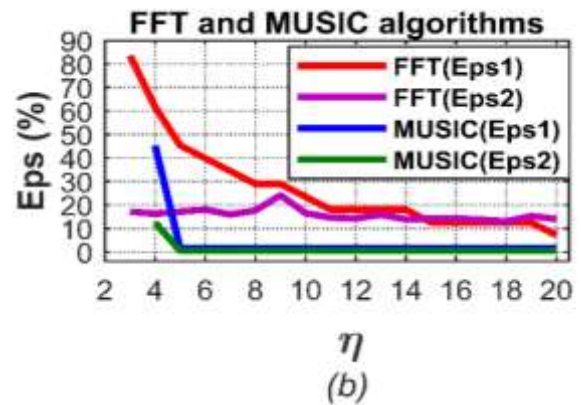


Fig. 6 (b) The relationship between the percentage error (E_{PS}) and η using the FFT and MUSIC algorithms $P_{S1} = 2$ cm, $P_{S2} =$ variable, $\gamma = 0.4$ cm, $\Delta s = 1$ cm, $\zeta = 70$ cm.

4.2 Results with noise:

When sending a wireless signal from T_x , it is exposed to AWGN noise (an unwanted effect that alters or distorts the signal) upon reception at R_x . Therefore, we will add this noise to the transmitted signal to study the impact of this issue on the results.

4.2.1 Simulation results with a single source:

Using the parameters $P_{S1} = 2$ cm, $\gamma = 0.4$ cm, $\Delta s = 1$ cm, $\zeta = 50$ cm, SNR = 5 dB, and $\eta = 10$, Fig. 7 shows that the FFT algorithm (red line) with added noise of SNR = 5 dB has $E_{PS} = 9.38\%$ in estimating the source

position with signal distortion and many and considerable SL levels.

In contrast, the MUSIC algorithm (blue line) with SNR = 5 dB achieves $E_{PS} = 6.25\%$ with the main lobe narrower compared to SNR = 5 dB (red line) and no SL levels.

This demonstrates that the MUSIC algorithm outperforms the FFT algorithm with a narrower main lobe, negligible SL levels, and lower E_{PS} .

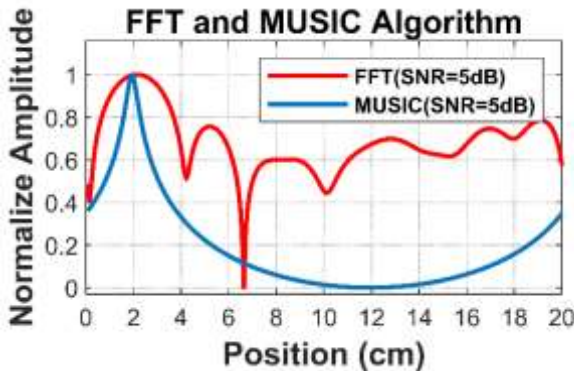


Fig. 7 Position estimation for a single source using the FFT and MUSIC algorithms $P_{S1} = 2$ cm, $\gamma = 0.4$ cm, $\Delta s = 1$ cm, $\zeta = 50$ cm, SNR = 5 dB, and $\eta = 10$.

Fig. 8 (a and b) illustrates the relationship between the percentage error (E_{PS}) and η for a single source at SNR = 5 dB after implementing the FFT and the MUSIC algorithms. The results showed that a decrease in SNR and η leads to an increase in E_{PS} . However, the MUSIC algorithm outperforms the FFT algorithm in reducing E_{PS} when estimating the source position.

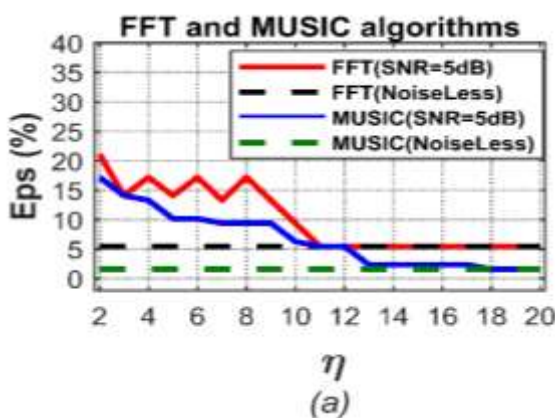


Fig. 8 (a) The relationship between the percentage error (E_{PS}) and η using the FFT and MUSIC algorithms $P_{S1} = 2$ cm, $\gamma = 0.4$ cm, $\Delta s = 1$ cm, $\zeta = 50$ cm, SNR = 5 dB.

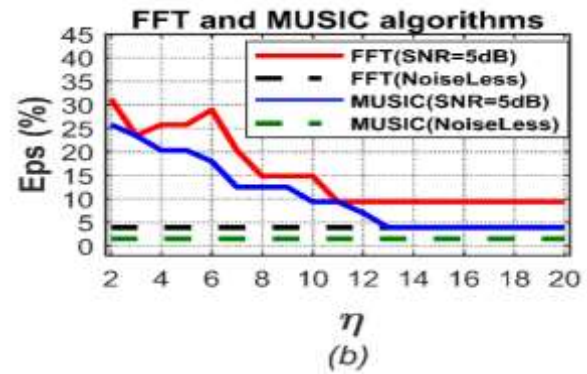


Fig. 8 (b) The relationship between the percentage error (E_{PS}) and η using the FFT and MUSIC algorithms $P_{S1} = 2$ cm, $\gamma = 0.4$ cm, $\Delta s = 1$ cm, $\zeta = 70$ cm, SNR = 5 dB.

4.2.2 Simulation results with two sources:

Using the parameter $P_{S1} = 2$ cm, P_{S2} is changed until obtaining a minimum detectable distance d_{pt} , $\gamma = 0.4$ cm, $\Delta s = 1$ cm, $\zeta = 50$ cm, SNR = 5 dB, and $\eta = 10$, Fig. 9 (a) shows that the FFT algorithm estimated the position of the first source at $P_{S1} = 1.641$ cm with $E_{PS1} = 17.97\%$, and $P_{S2} = 4.453$ cm with $E_{PS2} = 12.74\%$. It also distinguished between nearby sources with a distance of $d_{pt} = 1.95$ cm, with high SL levels and wide main lobes.

In contrast, Fig. 9 (b) shows that the MUSIC algorithm estimated the position of the first source at $P_{S1} = 1.797$ cm with $E_{PS1} = 10.16\%$, and $P_{S2} = 3.828$ cm with $E_{PS2} = 9.69\%$. It also distinguished between nearby sources with a distance of $d_{pt} = 1.49$ cm, with the main lobe narrower compared to Fig. 9 (a) and shallow SL levels.

This demonstrates that the MUSIC algorithm outperforms the FFT algorithm with a narrower main lobe, negligible SL levels, and lower E_{PS} .

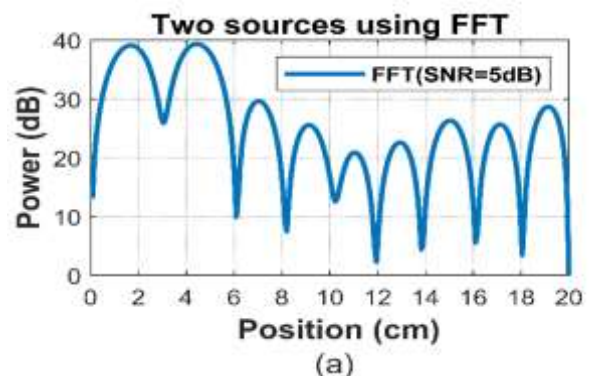


Fig. 9 (a) Position estimation for two sources using the FFT algorithms $P_{S1} = 2$ cm, $P_{S2} =$ variable, $\gamma =$

0.4 cm, $\Delta s = 1$ cm, $\zeta = 50$ cm, SNR = 5 dB, and $\eta = 10$.

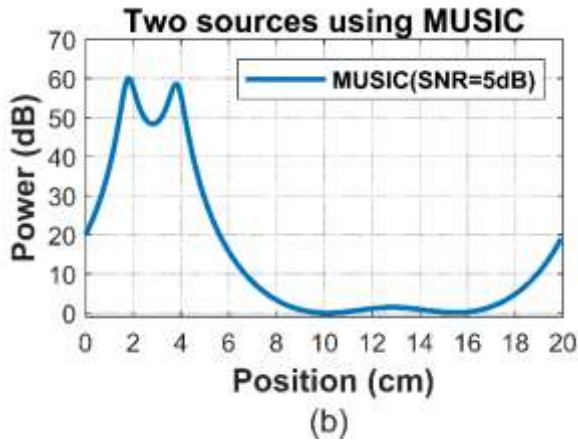


Fig. 9 (b) Position estimation for two sources using the MUSIC algorithms $P_{S1} = 2$ cm, $P_{S2} =$ variable, $\gamma = 0.4$ cm, $\Delta s = 1$ cm, $\zeta = 50$ cm, SNR = 5 dB, and $\eta = 10$.

After applying the FFT and MUSIC algorithms, Fig. 10 (a and b) illustrates the relationship between the minimum separation (dpt) and η for two sources in the presence of noise. Fig. 10 (a) illustrates the performance of the FFT algorithm. At the same time, Fig. 10 (b) shows that the MUSIC algorithm outperforms the FFT algorithm in Fig. 10 (a) by distinguishing very closely spaced sources (high resolution). The results indicate that dpt is affected by ζ , η , and SNR, increasing with ζ and lower SNR and decreasing with higher η .

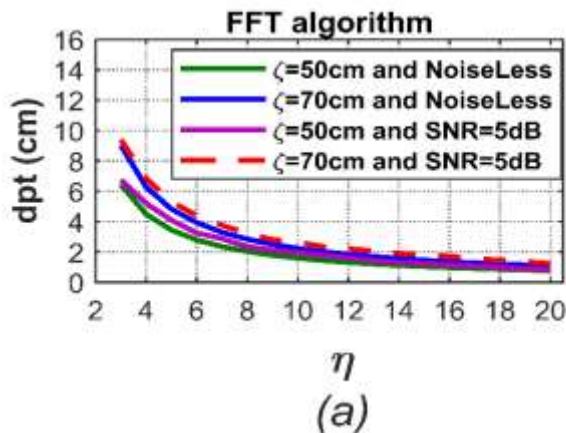


Fig. 10 (a) The relationship between minimum separation (dpt) and η using the FFT algorithm $P_{S1} = 2$ cm, $P_{S2} =$ variable, $\gamma = 0.4$ cm, $\Delta s = 1$ cm, SNR = 5 dB.

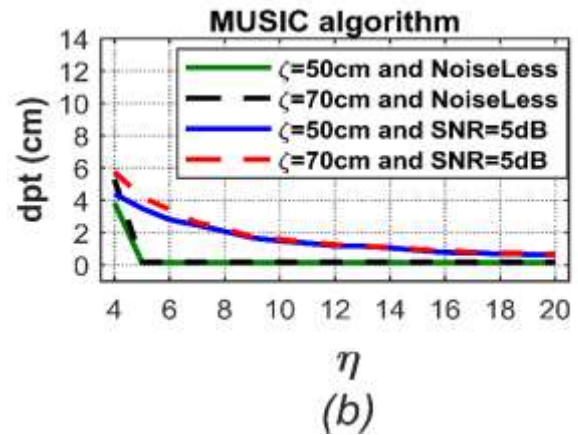


Fig. 10 (b) The relationship between minimum separation (dpt) and η using the MUSIC algorithm $P_{S1} = 2$ cm, $P_{S2} =$ variable, $\gamma = 0.4$ cm, $\Delta s = 1$ cm, SNR = 5 dB.

5 Conclusion

This research used the classical method, FFT, and the modern method, MUSIC, to estimate sources' positions with and without noise. Different parameters are used to study the performance of algorithms with the position estimation problem. Simulation results showed that with a single noise-free source, the MUSIC algorithm outperforms FFT in low percentage error, no side lobes, and narrow main lobe results. In the case of two noise-free sources, MUSIC also outperforms FFT in low percentage error, shallow side lobes, narrow main lobes, and high performance in distinguishing between sources that are very close to each other and estimating their positions (very small dpt). When implementing the algorithms with one and two sources with the noise, the results showed that the percentage error, side lobes, and dpt of FFT increase with decreasing SNR, while MUSIC remains superior and still performs better than FFT.

References:

- [1] R. Dastres and M. Soori, "A review in advanced digital signal processing systems," *Int. J. Electr. Comput. Eng.*, 2021.
- [2] J. D. Gibson, *Digital Communications: Introduction to Communication Systems*. Springer Nature, 2023.
- [3] Z. Ahmad, "Fundamentals of narrowband array signal processing," in *Adaptive Filtering-Recent Advances and Practical Implementation*, IntechOpen, 2021.

- [4] S. Mohammadi, A. Ghani, and S. H. Sedighy, "Direction-of-arrival estimation in conformal microstrip patch array antenna," *IEEE Trans. Antennas Propag.*, vol. 66, no. 1, pp. 511–515, 2017.
- [5] L. Osman, I. Sfar, and A. Gharsallah, "The application of high-resolution methods for DOA estimation using a linear antenna array," *Int. J. Microw. Wirel. Technol.*, vol. 7, no. 1, pp. 87–94, 2015.
- [6] B. P. Nxumalo, "Efficient method of estimating Direction of Arrival (DOA) in communications systems.," PhD Thesis, 2021.
- [7] H. Krim and M. Viberg, "Two decades of array signal processing research: the parametric approach," *IEEE Signal Process. Mag.*, vol. 13, no. 4, pp. 67–94, 1996.
- [8] M. V. Kraynyuk and O. K. Alsova, "Research of the synchronous spectral analysis method," in *2016 11th International Forum on Strategic Technology (IFOST)*, IEEE, 2016, pp. 449–450.
- [9] H. Wen, S. Guo, Z. Teng, F. Li, and Y. Yang, "Frequency estimation of distorted and noisy signals in power systems by FFT-based approach," *IEEE Trans. Power Syst.*, vol. 29, no. 2, pp. 765–774, 2013.
- [10] O. Martinez Manzanera, J. W. Elting, J. H. van der Hoeven, and N. M. Maurits, "Tremor detection using parametric and non-parametric spectral estimation methods: A comparison with clinical assessment," *PloS One*, vol. 11, no. 6, p. e0156822, 2016.
- [11] M. Behrendt, M. de Angelis, L. Comerford, Y. Zhang, and M. Beer, "Projecting interval uncertainty through the discrete Fourier transform: An application to time signals with poor precision," *Mech. Syst. Signal Process.*, vol. 172, p. 108920, 2022.
- [12] M. S. G. Jagtap and A. S. Kunte, "Improved Direction of Arrival Estimation using Multiple Signal Classification (MUSIC) Algorithm with Decomposition and Normalization," 2023.
- [13] Y. Liao, A. Abouzaid, and R. April, "Resolution Improvement for MUSIC and ROOT MUSIC Algorithms.," *J Inf Hiding Multim Signal Process*, vol. 6, no. 2, pp. 189–197, 2015.
- [14] P. Yadav and R. Mehra, "Power Spectrum Estimation for Narrowband and Broadband Applications using Subspace Method," *Int. J. Comput. Appl.*, vol. 130, no. 10, pp. 4–7, 2015.
- [15] B. Kim, J. Lee, S. Kim, and R. M. Narayanan, "MIMO Imaging Method with Extrapolation-Iterative Adaptive Approach-Based Super-Resolution Technique for Automotive Radar," in *2024 IEEE Radar Conference (RadarConf24)*, IEEE, 2024, pp. 1–6.
- [16] A. P. Anderson, "Microwave holography," *Proc. Inst. Electr. Eng.*, vol. 124, no. 11R, p. 946, 1977.
- [17] K. H. S. Marie, A. P. Anderson, and J. C. Bennett, "Digital in-line holographic techniques for long wavelength imaging," *IEE Proc. H Microw. Opt. Antennas*, vol. 129, no. 4, p. 211, 1982.
- [18] A. T. Qaba and M. F. Al-azo, "Improved resolution for separation between acoustical transmitters with their locations using Eigenvector algorithm," in *IOP Conference Series: Materials Science and Engineering*, IOP Publishing, 2021, p. 012029.
- [19] A. R. Kale, D. G. Ganage, and S. A. Wagh, "Subspace Based DOA Estimation Techniques." Volume, 2015.
- [20] X.-D. Zhang, *Modern signal processing*. Walter de Gruyter GmbH & Co KG, 2022.
- [21] S. Palani, *Principles of Digital Signal Processing: 2nd Edition*. Cham: Springer International Publishing, 2022.
- [22] J. G. Proakis, *Digital signal processing: principles, algorithms, and applications, 4/E*. Pearson Education India, 2007.
- [23] E. Kwizera, E. Mwangi, and D. Konditi, "Direction of arrival estimation based on MUSIC algorithm using uniform and non-uniform linear arrays," *Eva Kwizera Al Int J. Eng. Res. Appl.*, vol. 7, no. 3, pp. 51–58, 2017.
- [24] P. K. Eranti and B. D. Barkana, "An overview of direction-of-arrival estimation methods using adaptive directional time-frequency distributions," *Electronics*, vol. 11, no. 9, p. 1321, 2022.